doi:10.1093/brain/aww310 BRAIN 2017: 140; 414–428 | 414

BRAIN
A JOURNAL OF NEUROLOGY

Genetic inactivation of glutamate neurons in the rat sublaterodorsal tegmental nucleus recapitulates REM sleep behaviour disorder

Sara Valencia Garcia,[1,2] Paul-Antoine Libourel,[1,2] Michael Lazarus,[3] Daniela Grassi,[3] Pierre-Hervé Luppi[1,2] and Patrice Fort[1,2]

See Schenck and Mahowald (doi:10.1093/aww329) for a scientific commentary on this article.

Idiopathic REM sleep behaviour disorder is characterized by the enactment of violent dreams during paradoxical (REM) sleep in the absence of normal muscle atonia. Accumulating clinical and experimental data suggest that REM sleep behaviour disorder might be due to the neurodegeneration of glutamate neurons involved in paradoxical sleep and located within the pontine sublaterodorsal tegmental nucleus. The purpose of the present work was thus to functionally determine first, the role of glutamate sublaterodorsal tegmental nucleus neurons in paradoxical sleep and second, whether their genetic inactivation is sufficient for recapitulating REM sleep behaviour disorder in rats. For this goal, we first injected two retrograde tracers in the intralaminar thalamus and ventral medulla to disentangle neuronal circuits in which sublaterodorsal tegmental nucleus is involved; second we infused bilaterally in sublaterodorsal tegmental nucleus adeno-associated viruses carrying short hairpin RNAs targeting *Slc17a6* mRNA [which encodes vesicular glutamate transporter 2 (vGluT2)] to chronically impair glutamate synaptic transmission in sublaterodorsal tegmental nucleus neurons. At the neuroanatomical level, sublaterodorsal tegmental nucleus neurons specifically activated during paradoxical sleep hypersomnia send descending efferents to glycine/GABA neurons within the ventral medulla, but not ascending projections to the intralaminar thalamus. These data suggest a crucial role of sublaterodorsal tegmental nucleus neurons rather in muscle atonia than in paradoxical sleep generation. In line with this hypothesis, 30 days after adeno-associated virus injections into sublaterodorsal tegmental nucleus rats display a decrease of 30% of paradoxical sleep daily quantities, and a significant increase of muscle tone during paradoxical sleep concomitant to a tremendous increase of abnormal motor dream-enacting behaviours. These animals display symptoms and behaviours during paradoxical sleep that closely mimic human REM sleep behaviour disorder. Altogether, our data demonstrate that glutamate sublaterodorsal tegmental nucleus neurons generate muscle atonia during paradoxical sleep likely through descending projections to glycine/GABA premotor neurons in the ventral medulla. Although playing a role in paradoxical sleep regulation, they are, however, not necessary for inducing the state itself. The present work further validates a potent new preclinical REM sleep behaviour disorder model that opens avenues for studying and treating this disabling sleep disorder, and advances potential regions implicated in prodromal stages of synucleinopathies such as Parkinson's disease.

1 Neuroscience Research Center of Lyon (CRNL), CNRS UMR 5292, INSERM U1028, SLEEP Team, Lyon, France
2 Lyon1 Claude Bernard University, Lyon, France
3 International Institute for Integrative Sleep Medicine, University of Tsukuba, Tsukuba, Japan

Correspondence to: Dr Patrice Fort
Centre de Recherche en Neurosciences de Lyon (CRNL)
CNRS UMR5292 - INSERM U1028
Faculté de Médecine Lyon-Est – Laënnec/La Buire - UCBL 1

Received July 28, 2016. Revised September 14, 2016. Accepted October 14, 2016. Advance Access publication December 21, 2016

7, rue Guillaume Paradin 69372 LYON
Cedex 08 – France
E-mail: patrice.fort@univ-lyon1.fr

Keywords: REM sleep; Parkinson; REM sleep Behaviour Disorder; SLD; glutamate

Abbreviations: AAV = adeno-associated virus; CTb = cholera toxin b subunit; FG = FluoroGold®; RBD = REM sleep behaviour disorder; SLD = sublaterodorsal tegmental nucleus

Introduction

REM sleep behaviour disorder (RBD) is a parasomnia characterized by the loss of normal skeletal muscle atonia during paradoxical sleep (also coined REM sleep) favouring dream-enacting behaviours, without major modification of paradoxical sleep quantities (Schenck *et al.*, 1986). Recently RBD has been considered as a prodromal biomarker of synucleinopathies such as Parkinson's disease or multiple-system atrophy, resulting from pathological brain deposition of native α-synuclein protein (Iranzo *et al.*, 2013). Indeed, most patients (≈80%) diagnosed for RBD eventually develop one such synucleinopathy within 10–15 years (Iranzo, 2005; Postuma *et al.*, 2009; Iranzo *et al.*, 2013; Schenck, 2013). Neuroimaging and post-mortem studies recently observed damage or presence of Lewy bodies within the dorsal pontine tegmentum in patients with RBD and comorbid Parkinson's disease (Schenck *et al.*, 1996; Scherfler *et al.*, 2005; Tippmann-Peikert *et al.*, 2006; Mathis *et al.*, 2007; Boeve, 2013; Garcia-Lorenzo *et al.*, 2013; Iranzo *et al.*, 2013; Peever *et al.*, 2014). These data in humans suggest that loss of neurons in this area may be the primary cause of RBD pathogenesis. In fact, a small nucleus within the dorsal pons named sublaterodorsal tegmental nucleus (SLD, also coined subcoeruleus nucleus in humans and peri-locus coeruleus alpha in cats), seems crucial for muscle atonia during paradoxical sleep (Fort *et al.*, 2009; Luppi *et al.*, 2011; Peever *et al.*, 2014). Electrolytic or neurochemical lesion of SLD area induces in cats, rats and mice loss of muscle atonia, appearance of abnormal motor behaviours (muscle jerks of extremities, abrupt movements) and a reduction of paradoxical sleep amounts (Roussel *et al.*, 1976; Sastre and Jouvet, 1979; Lu *et al.*, 2006). Conversely, pharmacological activation of SLD neurons induces a paradoxical sleep-like state in cats (Vanni-Mercier *et al.*, 1989; Sakai *et al.*, 2001) and rats (Boissard *et al.*, 2002). Furthermore, the SLD contains neurons with a tonic firing activity highly specific to paradoxical sleep sending either ascending (to thalamus) or descending (to lower brainstem/spinal cord) projections (Sakai and Koyama, 1996; Boissard *et al.*, 2002; Sakai, 2015) and numerous c-Fos-labelled (c-Fos+) neurons after experimentally induced paradoxical sleep hypersomnia (Verret *et al.*, 2006; Sapin *et al.*, 2009; Clement *et al.*, 2011; Arthaud *et al.*, 2015). A vast majority (≈84%) of these neurons are glutamate as expressing the neuronal vesicular glutamate transporter 2 (vGluT2, encoded by *SLC17A6*; Clement *et al.*, 2011). We propose that entry in paradoxical sleep, marked by a synchronized cortical activation and muscle atonia, results from the strong activation of glutamate paradoxical sleep-on neurons circumscribed to the SLD (Luppi *et al.*, 2011). To further examine the specific role in paradoxical sleep of the glutamate SLD neurons in the rat, we first determined anatomically whether they provide projections both ascending (to the intralaminar thalamus) and descending (to the ventral gigantocellular reticular nucleus), the two main SLD targets (Boissard *et al.*, 2002). Then, we quantified the physiological effect on paradoxical sleep of bilateral infusion of adeno-associated viral vectors (AAVs) carrying short hairpin (sh)RNAs against *Slc17a6* (termed AAV-shvGluT2) to chronically inactivate glutamate neurotransmission from SLD neurons (Thakker *et al.*, 2006; Lazarus *et al.*, 2011). Combining molecular tools to innovative behavioural analysis methods, we demonstrate that selective glutamate transmission impairment in SLD is sufficient to mimic in healthy rats the major pathological symptoms of human RBD, i.e. a tremendous increase of abnormal motor behaviours, a nearly total loss of muscle atonia during paradoxical sleep with a limited decrease in paradoxical sleep quantities, explained by anatomical connections with inhibitory neurons in the ventral medulla. These original data unravel that glutamate SLD neurons generate the muscle atonia during paradoxical sleep but not the state of paradoxical sleep itself. Further, they validate a reproducible preclinical RBD model in rodents that may provide new experimental opportunities for clinical research to improve RBD treatments and thus patient's healthcare.

Materials and methods

Sprague Dawley male rats (Charles River Laboratories) were housed individually in recording Plexiglas® barrels (30 cm diameter, 40 cm height) under 12-h light/dark cycle (08:00 am/pm). Room temperature was maintained at 21 ± 1°C. Food pellets (A04 SAFE, Extra Labo) and water were available *ad libitum*.

Surgical procedures

Stereotaxic injection of cholera toxin b subunit and FluoroGold® retrograde tracers

Adult rats (280–290 g) were anaesthetized with a ketamine/xylazine mixture (100 and 50 mg/kg, respectively,

intraperitoneally; Virbac) and mounted in a stereotaxic frame (David Kopf Instruments). Two holes were drilled in the skull above the right gigantocellular reticular nucleus and intralaminar thalamus. A borosilicate glass micropipette (7–10 µm tip diameter) backfilled with low-salt cholera toxin b subunit (CTb; 0.5%; List Biological Laboratories; Luppi *et al.*, 1990) was lowered with hydraulic micropositioner (David Kopf Instruments) into the gigantocellular reticular nucleus [anterior-posterior (AP), −13.5 mm from Bregma; medial-lateral (ML), +1 mm; dorsal-ventral (DV), −8.5 mm below brain surface, 7° posterior angle; (Paxinos and Watson, 1998)]. The micropipette was connected by a silver wire to a current generator (CS4, Transkinetics) delivering a pulsed current (+1 µA, 7 s on/off) for 15 min. Similarly, a second micropipette backfilled with FluoroGold® (FG, 1%; Sigma-Aldrich) was lowered into intralaminar thalamus (AP, +3.7 mm from Bregma; ML, 0.8 mm; DV, 5 mm, 7° posterior angle) where FG was ejected using a constant current (+1 µA) for 15 min.

Stereotaxic injections of viral vectors

Young rats (240–260 g) were prepared in the same way for bilateral injections of viral vectors in SLD (AP, −10.9 mm to Bregma; ML, 1.2 mm; DV, 6.1 mm, 15° posterior angle). AAV-shvGluT2-mCherry and AAV-shCTRL-mCherry were injected with a cannula (33 gauge; PlasticsOne) connected by a polyethylene tubing (PlasticsOne) to a 10 µl Hamilton syringe placed into an UltraMicroPump (UMP3 with SYS-Micro4 controller, WPI). Each SLD received a volume of 300 nl delivered at 40 nl/min.

Surgical preparation for polysomnography

Once the injection procedure was completed, rats were implanted for polysomnographic recordings of cortical EEG and nuchal EMG (Verret *et al.*, 2005; Sapin *et al.*, 2009; Clément *et al.*, 2014; Renouard *et al.*, 2015). Briefly, four stainless-steel screws (PlasticsOne) were screwed to the skull over the frontal (AP, +3 mm to Bregma; ML, 1 mm), parietal (AP, −4 mm; ML, +3 mm), occipital (AP, −8 mm; ML, +3 mm) and cerebellar cortices (AP, −12 mm; ML, +3 mm; reference electrode). Two gold-coated electrodes were inserted in between neck muscles for differential EMG recording. Electrode leads were connected to a miniature plug (PlasticsOne) and fixed to the skull using acrylic Superbond (Sun Medical Co) and dental Paladur® cement (Heraeus Kuzler).

Generation of viral vectors

For the generation of AAV-shRNA-mCherry vector plasmids, a H1-shRNA-Ctrl cassette was amplified by polymerase chain reaction (PCR) from the pSilencer 3.1-H1 neoplasmid (Applied Biosystems, Life Tech) containing the control shRNA sequence (GTCAGGCTATCGCGTATCG; Ambion kit, Life Tech). This cassette was then inserted into the MluI site of the psiSTRIKE-hMGFP plasmid (Stratagene, Life Tech). Subsequently, the hrGFP gene was replaced by the mCherry encoding one. The sequence shCTRL was then removed via BamHI and HindIII and replaced by shRNA-vGluT2 sequence (TGAAACCAGAG ATAGCAAATC).

The AAVs of serotype rh10 were generated by tripartite transduction (AAV-rep2/caprh10 expression plasmid, adenovirus helper plasmid, and AAV-vector plasmid) into 293A cells. After 3 days, 293A cells were resuspended in artificial CSF, freeze-thawed four times and treated with benzonase nuclease (EMD Millipore) to degrade all forms of DNA and RNA. Subsequently, cell debris was removed by centrifugation and the virus titre in the supernatant was determined with quantitative PCR (AAV-shCTRL-mcherry, 4.5×10^{12} particles/ml and AAV-shvGluT2-mcherry, 5.6×10^{12} particles/ml).

Polysomnographic recordings

After 5–7 days to recover from surgery, rats were connected to a cable plugged to a rotating connector (PlasticsOne) allowing free movements. After 3 days of habituation, vigilance states were continuously recorded until the completion of experiments. EEG and EMG signals were amplified (MCP+, Alpha-Omega Engineering), analogue-to-digital converted with a sampling rate of 520.8 Hz and collected on a PC via a CED-1401 Plus interface with Spike2 software (CED). Polysomnographic recordings were synchronized to videos using digital black/white cameras (GigEPoE, Elvitec) managed by Streampix 6 software (NorPix).

Paradoxical sleep deprivation and recovery

Rats dedicated to tract-tracing studies were submitted before sacrifice to a selective paradoxical sleep deprivation with the standard flowerpot method (Maloney *et al.*, 1999; Verret *et al.*, 2005; Lu *et al.*, 2006; Sapin *et al.*, 2009; Clement *et al.*, 2011). Two experimental groups were made: (i) paradoxical sleep-deprived rats placed at 12:00 am for 75 h in a Plexiglas® barrel containing three platforms (6.5 cm in diameter) surrounded by water (2 cm); and (ii) paradoxical sleep hypersomniac rats submitted to the same protocol during 72-h and allowed to recover (paradoxical sleep rebound) in a barrel with a dry bed of woodchips. They were sacrificed 2 h after the first paradoxical sleep episode. During deprivation, food and water were available *ad libitum* and barrels were cleaned daily.

Histological procedures

Rats treated with viral vectors were sacrificed at Day 30 post-surgery and rats with retrograde tracers at Day 10–12 post-injection.

Preparation of brainstem sections

Under lethal anaesthesia with pentobarbital (150 mg/kg, intraperitoneally, Ceva Santé Animale), rats were transcardially perfused first with Ringer's lactate solution containing 0.1% heparin, followed by 500 ml of a cold fixative solution composed of 4% freshly depolymerized paraformaldehyde (PFA) in 0.1 M phosphate buffer pH 7.4. The brains were removed, placed overnight at 4°C in the same fixative and for 3 days in sterile 30% sucrose solution. Brains were then rapidly frozen in cooled methyl-butane and cut with a cryostat in serial coronal sections (25-µm thick for the tract-tracing studies and 30-µm thick for *in situ* hybridization). Serial free-floating sections were collected in RNase free cryoprotectant

solution and stored at −20°C until use (Sapin *et al.*, 2009; Clement *et al.*, 2011).

c-Fos/CTb, c-Fos/FG and CTb/FG double immunostaining

Free-floating sections were successively incubated in (i) a rabbit antiserum against c-Fos (1:10 000, Merck Millipore) or goat antiserum against CTb (1:80 000; List Biological Labs) in PBST-Az [phosphate-buffered saline (PBS) containing 0.3% Triton™ X-100 and 0.1% sodium azide] for 3 days at 4°C; (ii) biotinylated horse anti-rabbit or anti-goat IgG (1:1000 in PBST, Vector Labs) for c-Fos or CTb staining, respectively; and (iii) ABC-HRP solution (1:1000; Vectastain Elite kit, Vector Labs) for 90 min at room temperature. Finally, the staining was revealed in a 0.05 M Tris-HCl buffer, pH7.6, containing 0.25% 3,3′-diaminobenzidine-4HCl (DAB; Sigma-Aldrich), 0.03% H_2O_2 and 0.6% nickel ammonium sulphate. After extensive washes, the c-Fos immunostained sections were incubated in a rabbit antiserum against FG (1:20 000, Sigma-Aldrich); (ii) or a goat antiserum against CTb (1:80 000) in PBST-Az over 3 days at 4°C. Alongside, the CTb immunostained sections were incubated in a rabbit antiserum against FG (1:20 000) over 3 days at 4°C. Amplification steps were similar to those described above, except that the histochemical revelation was performed in DAB solution without nickel ammonium sulphate. In rats with a tracer injection in intralaminar thalamus, pontine sections were double immunostained for FG and choline acetyltransferase, a cholinergic marker (goat anti-ChAT, 1:5000; Chemicon). Finally, sections were mounted on glass slides, dried and coverslipped with Depex mounting medium.

In situ hybridization of *Slc17a6*/vGluT2 mRNA

Antisense and sense digoxigenin-labelled probes against *Slc17a6*/vGluT2 were synthesized from a recombinant linearized plasmid containing the *Slc17a6*/vGluT2 cDNA using a non-radioactive RNA labelling kit (Roche Diagnostic; Clement *et al.*, 2011). All buffers contained 0.2% of RNase inhibitor (ProtectRNA™, Sigma-Aldrich). Free-floating sections were firstly rinsed in PBST containing 10 mM dithiothreitol (DTT, Sigma-Aldrich) and a standard saline citrate solution (SSC 2×). They were then placed overnight at 65°C in the hybridization buffer containing 0.5 µg/ml of the digoxigenin-labelled probe. Sections were washed in SSC, 50% formamide, 0.1% Tween 20, treated with RNase A (USB Corporation) and finally incubated in a solution of anti-digoxigenin IgG conjugated to alkaline phosphatase (1:2000, Roche Diagnostic). Staining was revealed using nitroblue tetrazolium and 5-bromo-4-chloro-3-indolyl-phosphate (Roche Diagnostic). Finally, the sections were mounted on slides and coverslipped with VectaMount™ (Vector Labs). Controls in absence of anti-digoxigenin or with the sense probe were run to ensure for the labelling specificity.

mCherry immunohistochemistry and *in situ* hybridization for *Slc6a5*/GlyT2 mRNA

This protocol was designed to determine whether axons emanating from transducted SLD neurons contact ventral medullary glycine neurons. The antisense and sense digoxigenin-labelled probes against mRNA for *Slc6a5* (which encodes neuronal glycine transporter 2, GlyT2) were synthesized by reverse transcription from brainstem tRNA to obtain cDNA. This cDNA containing *Slc6a5*/GlyT2 sequence was linearized using a non-radioactive RNA labelling kit (Roche Diagnostic). The brain sections from AAV-treated rats were successively incubated overnight with a rat antiserum against mCherry (1:100 000 in PBST at 4°C, ThermoFisher Scientific), 90 min in biotinylated rabbit anti-rat IgG and in ABC-HRP (1:1000 in PBST; Vector Labs). Then, the sections were revealed for 15 min in a Tris-HCl containing 0.025% DAB and 0.003% H_2O_2. All buffers used contained 0.2% of RNase inhibitor (ProtectRNA, Sigma-Aldrich). Immunostained sections were then treated in the same way as for *Slc6a5*/GlyT2 probe. Controls of specificity were done by omitting the primary antibodies or by using the sense probe.

Double mCherry/vGluT2 immunofluorescence

Free-floating sections were incubated for 3 days at 4°C in PBST-Az containing both rabbit IgG against vGluT2 (1:500, Synaptic Systems) and rat IgG against mCherry (1:50 000, ThermoFisher Scientific). After rinses, they were incubated for 24 h in PBST containing a mixture of secondary donkey antibodies tagged with Alexa Fluor® 488 and 594 (anti-rabbit and anti-rat, respectively, 1:500, ThermoFisher Scientific). After rinses in PBST, sections were finally mounted on slides, coverslipped with Fluoromount™ (Vector Labs) and immediately analysed to prevent fluorescence fading. Digital images were scanned and recorded using a TCS-Sp5X confocal fluorescence microscope (Leica) at a resolution of 1024 × 1024 pixels/frame with an objective 63 × (zoom 3, 0.5 µm image thickness).

Analysis of polysomnographic data

Sleep quantification

Vigilance states were scored by 5-s epochs and classified as waking, slow-wave sleep and paradoxical sleep based on the visual inspection of EEG/EMG signals. During waking, activated low-amplitude EEG is accompanied by a sustained EMG activity with phasic bursts. Slow-wave sleep is characterized by high voltage EEG slow waves, spindles and the disappearance of phasic muscle activity. A decrease in the EEG amplitude associated with a flat EMG (muscle atonia) and a regular and pronounced theta rhythm (theta band activity, 4–8 Hz) indicates the onset of paradoxical sleep. Hypnograms were then drawn directly using a custom script in Spike2 (CED). The values were finally exported to calculate standard parameters for each vigilance state [quantities, percentage, number and bout duration expressed as mean ± standard error of the mean (SEM)].

EMG quantification

The muscle atonia is defined as a drastic and sustained reduction of muscle tone during paradoxical sleep compared to the preceding slow-wave sleep. We computed nuchal EMG signals to extract mean muscle tone values for each paradoxical sleep episode and the preceding slow-wave sleep bout. Only paradoxical sleep episodes longer than 45 s were considered, eliminating first and last 5 s of each bout to avoid transition states (slow-wave sleep–paradoxical sleep and paradoxical sleep–waking). Then a mean value of EMG during paradoxical sleep and slow-wave sleep was obtained based on all

considered episodes. This was done for each rat of both experimental groups over the 12-h light period of Day 30 post-surgery. To better illustrate installation or not of muscle atonia between slow-wave sleep and paradoxical sleep in both groups, we calculated the ratio EMG during slow-wave sleep versus EMG during paradoxical sleep.

Actimetry

Nuchal EMG does not reflect motor activity of distal extremities (limbs, ears, whiskers). We thus developed a MatLab routine to quantify whole body movements during consolidated paradoxical sleep episodes based on off-line videos synchronized to EEG/EMG recordings. This was done for each AAV-treated rat at Day 30 post-surgery during the 12-h light period. The so-called actimetric value represents the number of pixels with modified grey value between two successive video frames (20 ms interval) due to rat's movements. Finally, mean actimetric value was calculated for each paradoxical sleep episode for each animal as the mean pixels number modified per second during 12 h. To further estimate amounts of paradoxical sleep motor events, we defined in shCTRL rats the threshold as 99.5th percentile of mean actimetry value of consolidated paradoxical sleep bouts and then applied this threshold to paradoxical sleep episodes of shvGluT2 rats. In this way, we were able to calculate the number of motor events (defined as the pixels increase above the threshold and lasting > 50 ms) and the percentage of paradoxical sleep time that animals spend moving and twitching.

Spectral analysis

A fast Fourier transform (FFT) analysis of parietal EEG was computed using a Spike-2 script in shvGluT2 versus shCTRL rats across the 12-h light period on Day 30 post-surgery. All epochs with artefacts were excluded from the analysis. For each 5-s epoch, a power spectrum was calculated (bin size 0.2 Hz, 0–30 Hz). Then, a mean spectrum was generated for each vigilance state with standard frequency ranges of EEG rhythms (delta, 0.5–4.6 Hz; theta, 5.1–8.9 Hz; sigma, 9.9–14 Hz; beta, 15–30 Hz).

Quantitative analysis of CTb/FG, c-Fos/CTb and c-Fos/FG double-labelled neurons

We mapped singly labelled c-Fos (c-Fos+), CTb (CTb+) and FG (FG+) neurons and double-labelled CTb+/FG+, c-Fos+/CTb+ and c-Fos+/FG+ neurons in eight rats (four paradoxical sleep-deprived rats and four paradoxical sleep hypersomniac rats) with CTb and FG injection sites in the gigantocellular reticular nucleus and intralaminar thalamus of the same hemisphere. This analysis was focused on the dorsal pons, bilaterally from levels AP −8 to −9.4 mm to Bregma (Paxinos and Watson, 1998). Double-labelled sections taken every 200 µm were drawn and labelled cells plotted using an Axioskop microscope (Zeiss) equipped with a motorized *x*–*y*-sensitive stage and a colour video camera connected to a computerized image analysis system (Mercator; ExploraNova). Cells of each type (singly or double-labelled) were counted for each pontine area and exported using Mercator. When an area was present on several sections, neurons counted were summed.

Statistics

Because of the reduced number of animals used (3R principles in animal experiments), non-parametric statistical tests were used. For the comparison of vigilance states and numbers of labelled neurons across paradoxical sleep-deprived rats and paradoxical sleep hypersomniac rats conditions, Mann–Whitney U-test was used to identify pairwise differences. The effect of paradoxical sleep deprivation and recovery versus the baseline was analysed with a Wilcoxon signed rank test. Statistical differences in state quantities, duration, number and mean duration of episodes, spectral analysis, EMG quantification and actimetry in shCTRL versus shvGluT2 rats were also determined with a Mann–Whitney U-test. All statistics were performed using StatView software and a significant effect was considered when $P < 0.05$.

Animal studies approval

All experiments were conducted in application of the 3R principles in animal experiments and in accordance to the European Community Council Directive for the use of research animals (86/609/EEC; http://ec.europa.eu/food/fs/aw/aw_legislation/scientific/86-609-eec_en.pdf and 2010/63/EU; http://ec.europa.eu/environment/chemicals/lab_animals/pdf/endorsed_awb-nc.pdf). Protocols and procedures used were approved by the local Comité d'Ethique en Experimentation Animale of Lyon I University (C2EA-55, UCBL) and the French Ministère de l'Enseignement Supérieur et de la Recherche (Authorization number DR-2014-37).

Results

Are glutamate sublaterodorsal tegmental nucleus neurons in position to generate paradoxical sleep?

We hypothesized that paradoxical sleep (PS)-on (higher activity during paradoxical sleep) SLD neurons induce cortical activation via their projections to the intralaminar thalamus and muscle atonia by collaterals to ventral gigantocellular reticular nucleus (Boissard *et al.*, 2002; Luppi *et al.*, 2011). We first assessed whether the SLD contains CTb/FG double-labelled neurons after injections of CTb and FG retrograde tracers, respectively, in the right gigantocellular reticular nucleus and intralaminar thalamus ($n = 4$ rats, Fig. 1A). As illustrated in Fig. 1B, FG injections (400–500 µm in diameter) encroached both the central medial and mediodorsal intralaminar thalamus while CTb injection sites restricted to the gigantocellular reticular nucleus were smaller in diameter (200–250 µm; Fig. 1C). The analysis revealed an overlapped distribution of CTb+ and FG+ cell bodies within the dorsal pons. Indeed, numerous FG+ neurons were found with an ipsilateral predominance in the laterodorsal tegmental nucleus and to a lesser degree

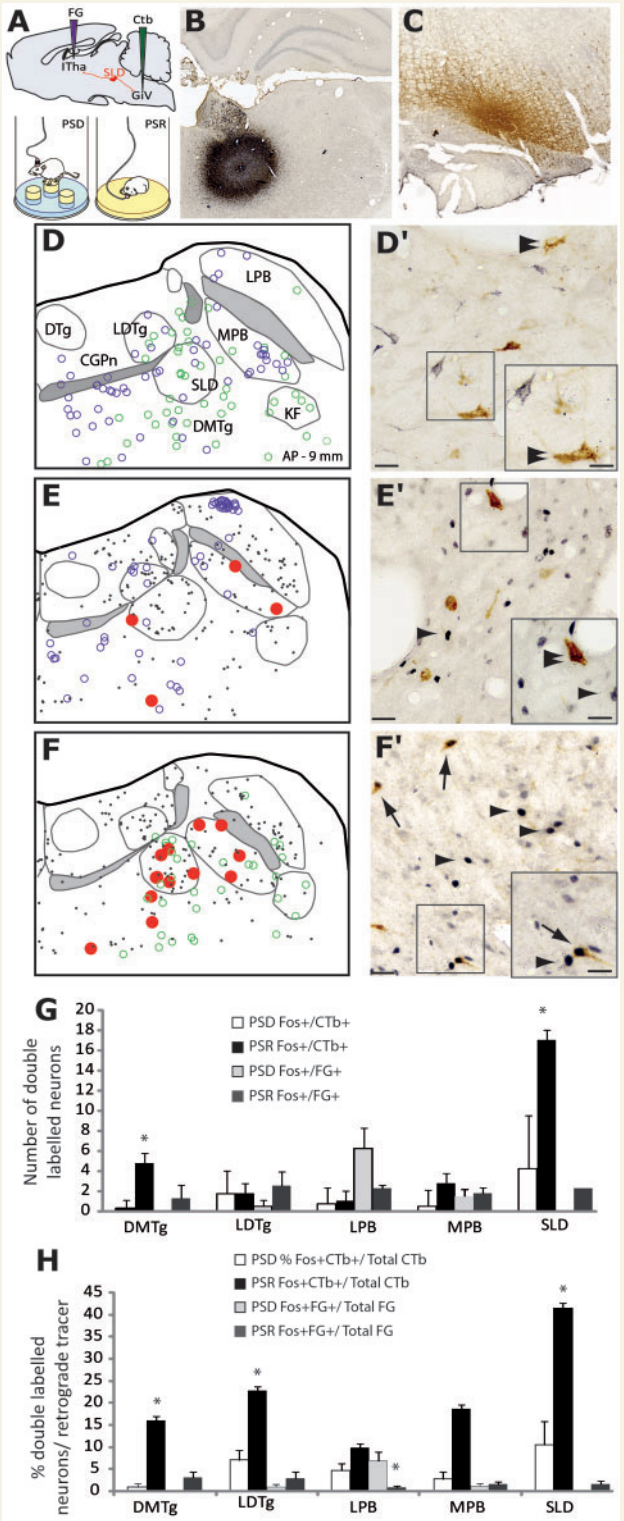

Figure 1 Glutamate SLD neurons activated during paradoxical sleep send descending projections to ventral medulla but not ascending efferents to the thalamus.
(**A**) Scheme of double-injection of CTb and FG in rats that were then submitted to 72-h protocol of paradoxical sleep deprivation (PSD) or paradoxical sleep rebound (PSR) using the flowerpot method. Photomicrographs illustrating representative injection sites of FluoroGold® in intralaminar thalamus (ITha) (**B**) and CTb in gigantocellular reticular nucleus (GiV) (**C**). (**D**) Drawings showing the SLD and the dorsomedial tegmental area just ventral to it. Conversely, CTb + cells were more abundant in ipsilateral SLD and dorsomedial tegmental area than in laterodorsal tegmental nucleus (Fig. 1D, D' and Table 1). Despite the overlapping distribution of CTb + and FG + neurons, double-labelled cells were never observed within the SLD, laterodorsal tegmental nucleus and dorsomedial tegmental area (Fig. 1D and D') or in other brain areas (not shown). These anatomical data reveal that SLD ascending and descending projections emanate from two distinct intermingled cell subpopulations and not a single one as anticipated.

To determine if these pathways are activated during paradoxical sleep, rats with an injection of CTb into the gigantocellular reticular nucleus ($n = 8$; Fig. 1B) or FG into

Figure 1 Continued
the distribution in SLD and neighbouring pontine areas of the CTb + (green circles) and FG + neurons (violet circles). No double-labelled neurons were countered in these areas including SLD despite no separation pattern between both populations of retrogradely-labelled neurons. (**D'**) Low- and higher- (framed area) power photomicrographs showing both populations of neurons retrogradely-labelled within the SLD. (**E**) Drawings illustrating the distribution of single FG + (violet circles, brown cytoplasmic staining), single c-Fos + (black dots, black nuclear staining), double-labelled c-Fos + /FG + neurons (red dots) within the SLD area. (**E'**) Low- and higher- (framed area) power photomicrographs showing very few SLD neurons active after paradoxical sleep rebound and projecting to intralaminar thalamus. (**F**) Schematic distributions of single- CTb + (green circles, brown cytoplasmic staining), single- c-Fos + (black dots, black nuclear staining) and double-stained c-Fos + /CTb + neurons (red dots) within SLD area. (**F'**) Low- and higher- (framed area) power photomicrographs showing the high number of paradoxical sleep active neurons and projecting to gigantocellular reticular nucleus. Arrows pointed out double-stained neurons (c-Fos + /FG + or c-Fos + /CTb +), arrowheads singly c-Fos + and double arrowhead singly CTb + or FG + . (**G**) Histogram showing the numbers of double-labelled neurons within the SLD and neighbouring pontine areas for each retrograde tracer used (CTb, FG) and experimental conditions [paradoxical sleep-deprived rats ($n = 4$) and paradoxical sleep hypersomniac rats ($n = 4$)]. Only SLD and dorsomedial tegmental area (DMTg) depicted significantly higher numbers of neurons activated during paradoxical sleep and projecting to the gigantocellular reticular nucleus (c-Fos + /CTb + neurons) in paradoxical sleep hypersomniac versus paradoxical sleep-deprived rats condition. (**H**) Percentage of double-labelled (single CTb + or single FG +) neurons within SLD and neighbouring pontine areas for each experimental condition (paradoxical sleep-deprived rats, $n = 4$; paradoxical sleep hypersomniac rats, $n = 4$). Percentages calculated for SLD, laterodorsal tegmental nucleus and dorsomedial tegmental area are significantly higher in paradoxical sleep hypersomniac rats compared to paradoxical sleep-deprived rats. LDTg = laterodorsal tegmental nucleus; LPB = lateral parabrachial nucleus; MPB = medial parabrachial nucleus. *$P < 0.05$. Scale bars = 50 and 20 μm for low and high power photomicrographs, respectively.

Table 1 Glutamate SLD neurons activated during paradoxical sleep do not send collaterals to ventral medulla and thalamus

	n		DMTg 5	LDTg 5	LPB 5	MPB 5	SLD 5
FG +		Ipsi	11 ± 8.7	39.3 ± 6.9	48 ± 12.7	13.5 ± 5.4	17.8 ± 5.7
		Contra	2.25 ± 1.3	16.8 ± 4.6	27.3 ± 7.1	4.75 ± 2	7.25 ± 2
Fos + /FG +	PSD	Ipsi	0 ± 0	0.5 ± 0.3	6.3 ± 2.5	1.5 ± 1.2	0 ± 0
		Contra	0 ± 0	0.3 ± 0.3	5.0 ± 2.1	2.3 ± 2.3	0 ± 0
	PSR	Ipsi	1.3 ± 0.6	2.5 ± 1.3	2.3 ± 1.3	1.8 ± 0.9	0 ± 0
		Contra	0.8 ± 0.5	0.8 ± 0.3	1.5 ± 0.6	0 ± 0	2.3 ± 1.1
% doubles/total FG	PSD	Ipsi	0 ± 0	1.0 ± 0.6	6.9 ± 2.0	1.1 ± 0.6	0.3 ± 0.3
		Contra	0 ± 0	0.9 ± 0.9	10.5 ± 3.7	1.5 ± 1.5	0 ± 0
	PSR	Ipsi	2.9 ± 1	4.2 ± 2.7	4 ± 1.8	7.8 ± 3	6 ± 2.5
		Contra	1.2 ± 0.8	1.8 ± 0.8	3.1 ± 1.7	0.0 ± 0.0	1.1 ± 1.1
% doubles FG/total Fos	PSD	Ipsi	0 ± 0	2.1 ± 1.3	3 ± 1.2	7.5 ± 5.1	0 ± 0
		Contra	0 ± 0	0.6 ± 0.6	2.6 ± 1.2	7.5 ± 7.5	0 ± 0
	PSR	Ipsi	3.0 ± 1.3	2.8 ± 1.4	0.8 ± 0.4	1.6 ± 0.6	1.6 ± 0.7
		Contra	1.2 ± 0.8	0.8 ± 0.3	0.5 ± 0.2*	0 ± 0	0.2 ± 0.2
CTb +		Ipsi	30.5 ± 7.2	14 ± 1.5	21 ± 6.7	25.5 ± 5.8	38 ± 9.7
		Contra	24 ± 3.8	8 ± 0.4	11.3 ± 1.7	10.8 ± 3.5	22.5 ± 4.3
Fos + /CTb +	PSD	Ipsi	0.3 ± 0.3	1.8 ± 0.8	0.8 ± 0.3	0.5 ± 0.3	4.3 ± 1.7
		Contra	0.8 ± 0.5	0 ± 0	1.3 ± 0.6	0.5 ± 0.5	1.8 ± 1.2
	PSR	Ipsi	4.8 ± 2.3	1.8 ± 0.5	1.0 ± 0.7	2.8 ± 1.5	17.0 ± 4.5
		Contra	8.3 ± 6	0.8 ± 0.5	2.0 ± 1.1	1.0 ± 0.6	7.5 ± 3.1*
% doubles/total CTb	PSD	Ipsi	0.9 ± 0.9	7.1 ± 2.3	4.7 ± 1.6	2.7 ± 1.6	10.5 ± 5.2
		Contra	2.1 ± 1.2	0.0 ± 0.0	13.7 ± 4.7	3.1 ± 3.1	4.1 ± 2.4
	PSR	Ipsi	16.0 ± 5.0	22.7 ± 9.2*	9.8 ± 8.0	18.5 ± 9.1	41.6 ± 11.1*
		Contra	17.2 ± 11.6	7.3 ± 4.8	19.2 ± 9.0	19.6 ± 12.2	23.8 ± 10.4
% doubles CTb/total Fos	PSD	Ipsi	2.8 ± 2.8	4.8 ± 1.0	0.8 ± 0.4	1.9 ± 1.1	10.5 ± 3.8
		Contra	8.6 ± 5.1	0.0 ± 0.0	1.0 ± 0.5	3.3 ± 3.3	3.1 ± 2.1
	PSR	Ipsi	8.8 ± 3.8	6.3 ± 3.5	1.8 ± 1.4	9.3 ± 7.1	19.1 ± 3.7
		Contra	10.4 ± 4.3	5.4 ± 4.9	1.2 ± 0.6	0.9 ± 0.5	12.7 ± 8.2

Mean numbers (mean ± SEM) of single FG + , single CTb + , double-labelled c-Fos + /FG + and double-labelled c-Fos + /CTb + neurons counted in the ipsilateral and contralateral SLD and neighbouring nuclei in paradoxical sleep-deprived rats ($n = 4$) and paradoxical sleep hypersomniac rats ($n = 4$) rats. For each rat and each pontine nucleus considered, sums of labelled neurons were calculated on five consecutive sections (200 μm interval) and then averaged for each rat's sample. The percentages displayed correspond to the ratio double- versus single-labelled neurons with each given marker of interest. For comparison between paradoxical sleep-deprived rats and paradoxical sleep hypersomniac rats condition, significance values after non-parametric unpaired Mann-Whitney U-test are given by $^*P < 0.05$. DMTg = dorsomedial tegmental area; LDTg = laterodorsal tegmental nucleus; LPB = lateral parabrachial nucleus; MPB = medial parabrachial nucleus; PSD = paradoxical sleep deprivation; PSR = paradoxical sleep rebound.

the intralaminar thalamus ($n = 8$, Fig. 1A) were submitted to the flowerpot method of paradoxical sleep deprivation. Half of the animals sacrificed after 72-h of paradoxical sleep deprivation (the paradoxical sleep-deprived rats group) spent 3.8 ± 1.3% of their time in paradoxical sleep (versus 14.5 ± 1.5% in baseline) during the last 2 h before sacrifice. The remaining rats (the paradoxical sleep hypersomniac rats group) were allowed to recover for 2 h during which they displayed 35.3 ± 3.9% of paradoxical sleep (versus 15.8 ± 1.2% at baseline; Supplementary Table 1). In line with our previous studies, significantly higher numbers of c-Fos + neurons were found in the laterodorsal tegmental nucleus, dorsomedial tegmental area and SLD in paradoxical sleep hypersomniac versus paradoxical sleep-deprived rats (Fig. 1E and F). A significantly higher number of c-Fos + /CTb + neurons populated these structures in paradoxical sleep hypersomniac versus paradoxical sleep-deprived rats (Mann–Whitney U-test, $Z = -2.165$, $P = 0.03$; $Z = -2.304$, $P = 0.02$, respectively; Fig. 1G and Table 1). Within the SLD, the number of c-Fos + /CTb + neurons was of 17 ± 4.5 in paradoxical sleep hypersomniac rats rats (42% of CTb + neurons) versus 4.3 ± 1.7 (10.5% of CTb + neurons) in paradoxical sleep-deprived rats rats (Fig. 1F, F', H and Table 1) (Mann–Whitney U-test, $Z = -2\,021$, $P = 0.04$). By comparison, 22% and 16% of the CTb + cells within laterodorsal tegmental nucleus (1.8 ± 0.5) and dorsomedial tegmental area (4.8 ± 2.3) were c-Fos + in paradoxical sleep hypersomniac rats. In sharp contrast, after injection of FG into the intralaminar thalamus, c-Fos + /FG + neurons were rarely counted in the

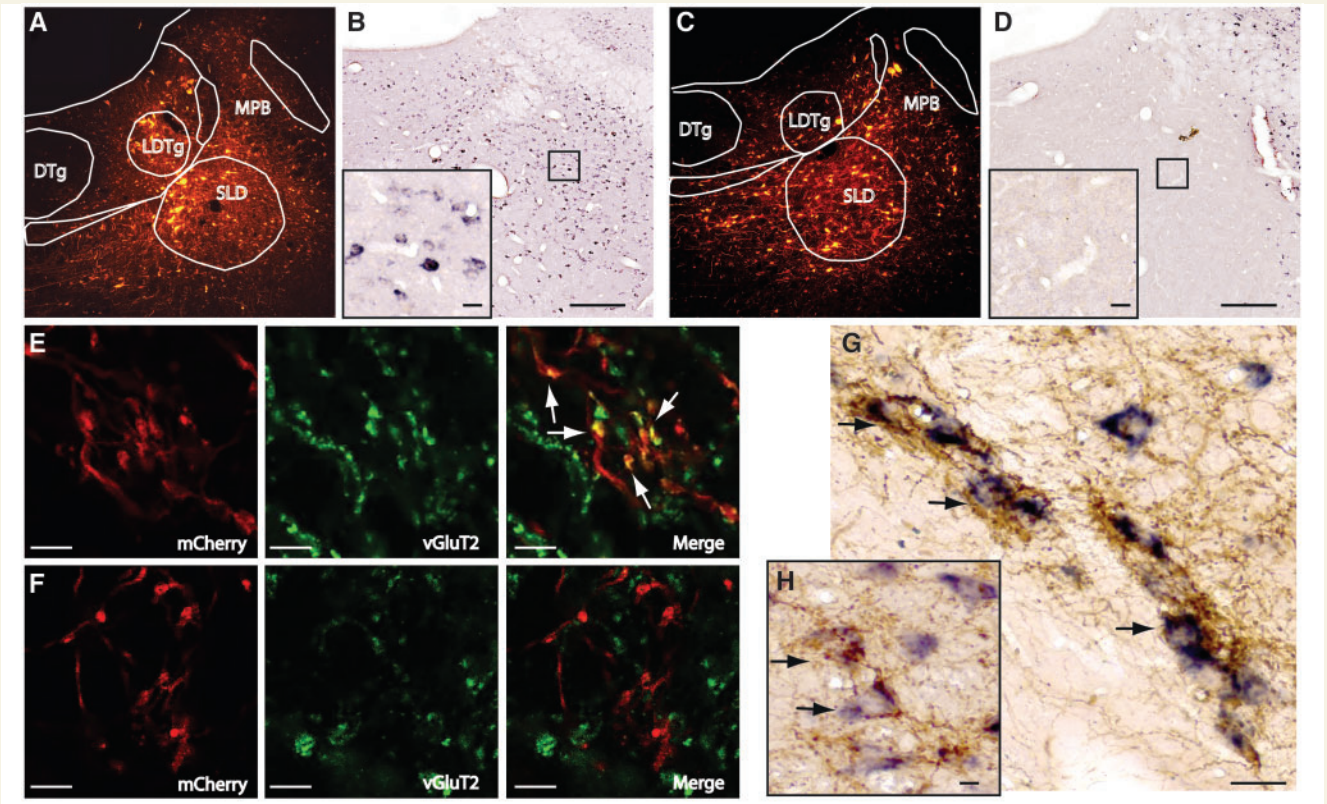

Figure 2 Verification of the genetic inactivation of vGluT2 in glutamate SLD neurons. Low power photomicrographs of the spontaneous mCherry fluorescence that delineates the AAV injection sites targeted SLD area of a representative AAV-shCTRL (**A**) and AAV-shvGluT2 and (**C**) rats. Note the presence in both cases of high numbers of transducted mCherry-fluorescent neurons within the injection sites. Low and higher (enlargement) power photomicrographs of adjacent sections treated for *Slc17a6*/vGluT2 *in situ* hybridization from the same AAV-shCTRL (**B**) and AAV-shvGluT2 (**D**) rats. Note the absence of *Slc17a6*/vGluT2 mRNA expression within the boundaries of viral spread in AAV-shvGluT2 rats. Confocal photomicrographs comparing in the gigantocellular reticular nucleus (GiV) the expression of native vGluT2 protein (green-immunofluorescent, *middle*) in synaptic terminals emanating from transducted SLD neurons (mCherry-fluorescent, *left*) in the same representative AAV-shCTRL (**E**) and AAV-shvGluT2 (**F**) animals. Note that native vGluT2 protein, while expressed in axons (arrowheads) emanating from SLD neurons in AAV-shCTRL rats (yellow fluorescence in **E**, *right*) is virtually absent in gigantocellular reticular nucleus of AAV-shvGluT2 rats (**F**, *right*). Photomicrographs showing that SLD efferent fibres immunolabelled for mCherry (coloured in brown) contact directly GlyT2-expressing neurons (*in situ* hybridization blue cytoplasmic staining) in the gigantocellular reticular nucleus (**G**) and neighboring raphe magnus (RMg) (**H**). Scale bars = 200 μm in **A–D**; 20 μm in enlarged squares, **G** and **H**; 5 μm in **E** and **F**. DTg = dorsal tegmental area; LDTg = laterodorsal tegmental nucleus; MPB = medial parabrachial nucleus.

laterodorsal tegmental nucleus, dorsomedial tegmental area and SLD both in paradoxical sleep-deprived and hypersomniac rats (Fig. 1E, E' and Table 1). The lateral parabrachial nucleus (LPB) was the only structure in which the number of c-Fos+/FG+ neurons was different in paradoxical sleep-deprived versus paradoxical sleep hypersomniac rats (6.9 ± 2 versus 0.8 ± 0.4 of double-labelled neurons; $10.5 \pm 3.7\%$ versus $0.5 \pm 0.2\%$; Mann–Whitney U-test, $Z = -2.309$, $P = 0.02$) (Fig. 1G, H and Table 1). Further, we quantified that $23.6 \pm 4.3\%$ of FG+ neurons in SLD were immunopositive for ChAT ($n = 6$ rats). In conclusion, the functional heterogeneity of SLD neurons is not in favour of a single population of SLD neurons responsible for the synchronized induction of muscle atonia and EEG activation during paradoxical sleep, but more in position to generate muscle atonia during paradoxical sleep through excitatory descending inputs.

shRNA-vGluT2 suppresses glutamate signalling in the sublaterodorsal tegmental nucleus

To block synaptic glutamate release in SLD neurons, we performed local and bilateral injections of AAV-shvGluT2-mCherry (versus AAV-shCTRL-mCherry). Numerous SLD cell bodies were strongly fluorescent for mCherry (Fig. 2A–C) in injection loci in both experimental ($n = 5$) and control ($n = 5$) rats. We then assessed by *in situ* hybridization the expression/absence of *Slc17a6*/vGluT2 mRNA within AAV injection sites at Day 30 post-injection. In AAV-shCTRL rats, there were a large number of neurons expressing *Slc17a6*/vGluT2 mRNA (vGluT2+; Fig. 2B; Clement *et al.*, 2011) within the injection loci.

In AAV-shvGluT2, no vGluT2 + neurons were longer visible within the injection sites, highly contrasting with surrounding regions unaffected by AAVs spreading (Fig. 2D). Such total suppression of *Slc17a6*/vGluT2 mRNA expression was already achieved at Day 10 post-infusion (not shown) and no recovery was noticed at Day 30 post-treatment (Fig. 2C–D'). To control that native vGluT2 protein was indeed absent from the transducted glutamate SLD neurons, we examined by confocal microscopy in control and experimental rats the co-localization of vGluT2 and mCherry in axon terminals in ventral medulla including raphe magnus, alpha gigantocellular reticular nucleus and gigantocellular reticular nucleus. In control rats, a high number of mCherry-labelled fibres and terminals (red) were also stained for vGluT2 (green) and thus appeared yellow coloured on merge photomicrographs (Fig. 2E and F). In AAV-shvGluT2 animals, a dense plexus of mCherry-labelled fibres was also observed in raphe magnus, alpha gigantocellular reticular nucleus and gigantocellular reticular nucleus but no yellow labelling was detected on merged photomicrographs (Fig. 2F), indicating that the expression of vGluT2 is suppressed in transducted glutamate SLD neurons in AAV-shvGluT2 rats. By coupling the immunodetection of mCherry to the *in situ* hybridization for *Slc6a5*/GlyT2 mRNA, we observed plexuses of mCherry-labelled fibres closely apposed on GlyT2 + neurons in raphe magnus, alpha gigantocellular reticular nucleus and gigantocellular reticular nucleus (Fig. 2G and H). Taken together, our data indicate that glutamate release of SLD neurons in their synaptic terminals in proximity of GABA/glycine neurons within the ventral medulla is chronically prevented in AAV-shvGluT2 rats.

Glutamate sublaterodorsal tegmental nucleus neurons are not necessary for paradoxical sleep generation

To study the role of glutamate SLD neurons in paradoxical sleep, we compared the sleep–waking cycle of AAV-shvGluT2 and AAV-shCTRL rats at Day 30 post-treatment. As shown in Fig. 2A–C, injection sites (< 800 µm in diameter) embraced the whole SLD, only slightly encroaching adjacent pontine areas such as the ventral part of laterodorsal tegmental nucleus or the dorsomedial tegmental area. Only treated rats depicting bilateral AAVs injections centred and covering the whole SLD were included in this study ($n = 5$ rats in each group; Fig. 3A).

Daily paradoxical sleep quantities were significantly reduced (−33%) in experimental versus control rats (7.3 ± 1.7 versus 10.9 ± 0.6% of total time; Mann–Whitney U-test, $Z = -2.008$, $P = 0.04$; Fig. 3B). The decrease was due to a non-significant reduction of both the number (99.4 ± 23.7 versus 108.8 ± 16.2, $P = 0.60$) and duration of paradoxical sleep bouts (1.0 ± 0.1 versus 1.6 ± 0.6 min, $P = 0.07$, Supplementary Table 2). Daily slow-wave sleep amounts showed a tendency to decrease in experimental rats (39.7 ± 2.9 versus 33.4 ± 3.2%; $P = 0.23$) counterbalanced by a non-significant increase of daily waking amounts (49.4 ± 2.9 versus 59.3 ± 4.7%; $P = 0.068$; Fig. 3B and Supplementary Table 2). No significant difference in EEG power spectrum was evidenced during paradoxical sleep between the two groups (Fig. 3C). In summary, genetic inactivation of glutamate SLD neurons induces a limited decrease of paradoxical sleep quantities, not supporting the consensual hypothesis that these neurons are responsible for paradoxical sleep generation. This is in line with our preceding neuroanatomical and functional data that glutamate PS-on SLD neurons do not send ascending projections and are hence not in a suitable position for synchronizing the generation of paradoxical sleep *per se*.

Glutamate sublaterodorsal tegmental nucleus neurons are responsible for muscle atonia during paradoxical sleep

As shown by nuchal EMG recordings in AAV-shCTRL rats (Fig. 3D), muscle atonia is defined as a sustained decrease of the muscle tone during paradoxical sleep compared to the preceding slow-wave sleep episode. This contrasts with EMG recordings in AAV-shvGluT2 rats showing alternating periods of high to low muscle tone along paradoxical sleep episodes and an increase of excessive, abnormal and sporadic motor activities (Fig. 3E and F). To compare muscle tone, we calculated at Day 30 the mean amplitude of the EMG signal during paradoxical sleep and prior slow-wave sleep episodes. In AAV-shCTRL rats, a significant decrease of absolute EMG values was observed during paradoxical sleep compared to slow-wave sleep (8.6 ± 0.9 versus 9.7 ± 0.9 respectively; Wilcoxon test, $P = 0.04$) resulting in a mean paradoxical sleep versus slow-wave sleep ratio of 0.91, indicative for a lower nuchal muscle tone during paradoxical sleep than during slow-wave sleep (Fig. 3G and H). In contrast, AAV-shvGluT2 rats did not show significant difference of absolute EMG values during paradoxical sleep and prior slow-wave sleep (12.6 ± 1.6 versus 11.6 ± 2.0; Wilcoxon test, $P = 0.14$). Further, the mean ratio value was slightly superior to 1 (1.03) and significantly higher in experimental versus control rats (Mann–Whitney U-test, $Z = -2.739$, $P = 0.02$; Fig. 3F and G). Indeed, no difference in absolute EMG values was observed during slow-wave sleep between the two groups of rats (Mann–Whitney U-test, $Z = -1.149$, $P = 0.25$, Fig. 1G), or in the duration of phasic bursts (0.81 ± 0.13 in experimental versus 0.61 ± 0.09 s in control rats; Mann-Whitney U-test Z-value = −1.149; $P = 0.2506$).

Nevertheless, nuchal EMG recordings do not reflect the occurrence of remarkable phasic motor events during paradoxical sleep in AAV-shvGluT2 rats at the level of extremities such as limbs, tail or face (Fig. 3D–F and

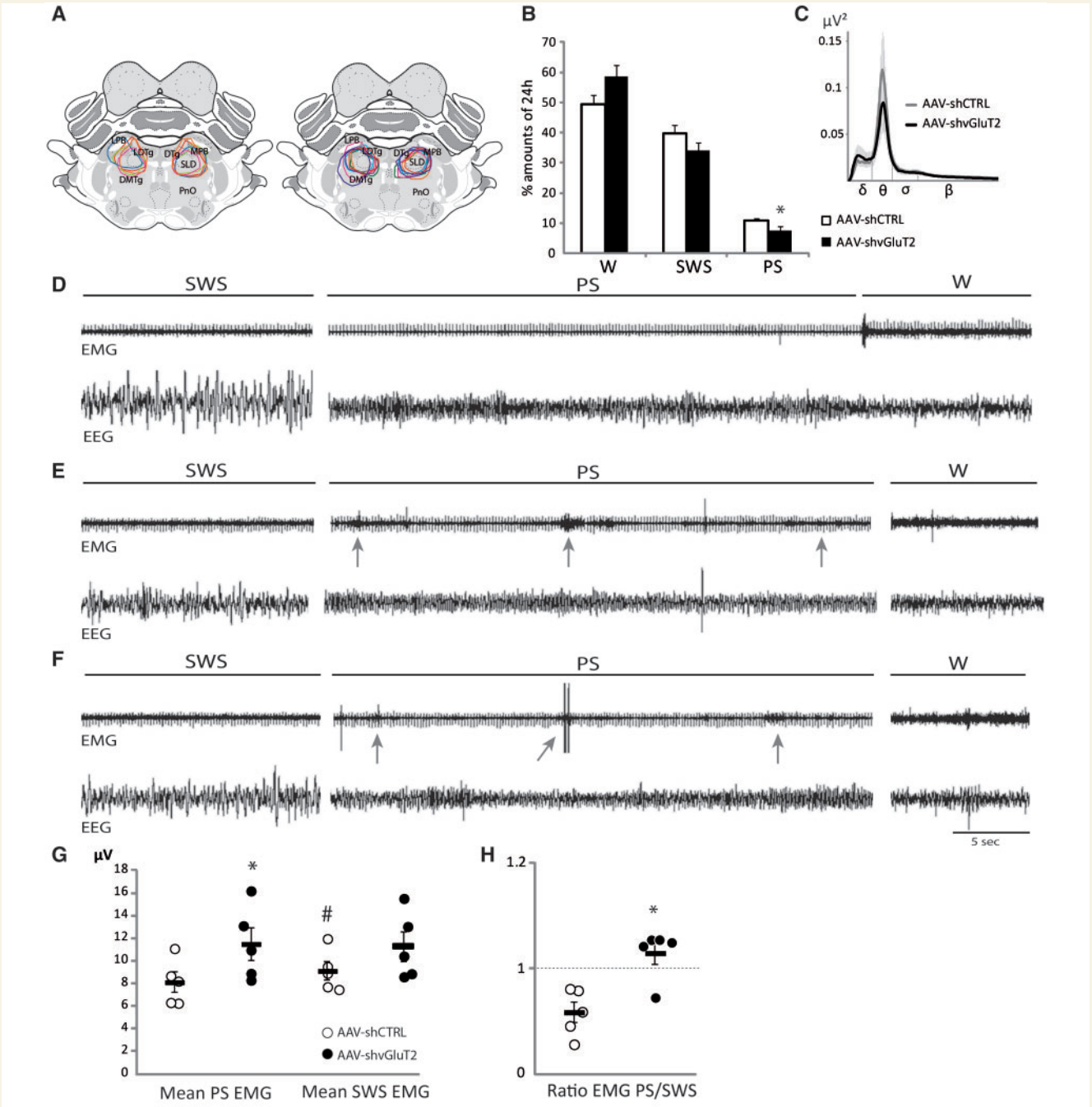

Figure 3 Atonia during paradoxical sleep disappeared after genetic inactivation of glutamate SLD neurons. (**A**) Schematic illustrating the location of AAV injection sites in representative AAV-shCTRL (*left*) and AAV-shvGluT2 (*right*) rats according to the spontaneous emitted fluorescence of mCherry reporter protein. Only animals with AAV injections bilaterally centred on SLD were considered for the physiological study (n = 5 for each group). (**B**) Histogram comparing the daily percentages of waking (W), slow-wave sleep (SWS) and paradoxical sleep in AAV-shCTRL (open bars) versus AAV-shvGluT2 (filled bars) rats at Day 30 after AAV injections. Notice that paradoxical sleep amounts are reduced in experimental versus control rats. (**C**) Power spectrum of EEG during paradoxical sleep between both groups of rats is virtually identical. (**D**) Typical EMG/EEG recordings during slow-wave sleep, paradoxical sleep and waking in a control rat. (**E** and **F**) Polysomnographic recordings from a rat with genetic inactivation of glutamate SLD neurons showing normal slow-wave sleep and transition into paradoxical sleep. Notice, however, during paradoxical sleep irregular enhancements of EMG tone (arrows) and only brief periods of atonia. EMG tone during slow-wave sleep and waking remained normal. (**G**) Dot plots comparing mean EMG values during paradoxical sleep and slow-wave sleep in AAV-shCTRL (open circles) versus AAV-shvGluT2 (filled circles) rats. Control rats show a physiological diminution of mean EMG values during paradoxical sleep compared to preceding slow-wave sleep (i.e. paradoxical sleep atonia). In contrast, mean EMG values during paradoxical sleep and slow-wave sleep are comparable, not diminished, in experimental rats indicating that atonia is abolished. (**H**) Dot plots showing that paradoxical sleep:slow-wave sleep ratio of mean EMG values is increased in experimental (filled circles) versus control (open circles) rats. Mann-Whitney U-test, $^{*}P < 0.05$ compared to AAV-shCTRL; Wilcoxon test, $^{\#}P < 0.05$ compared to mean EMG values during paradoxical sleep. DTg = dorsal tegmental area; LDTg = laterodorsal tegmental nucleus; MPB = medial parabrachial nucleus; PnO= pontine reticular nucleus, oral part.

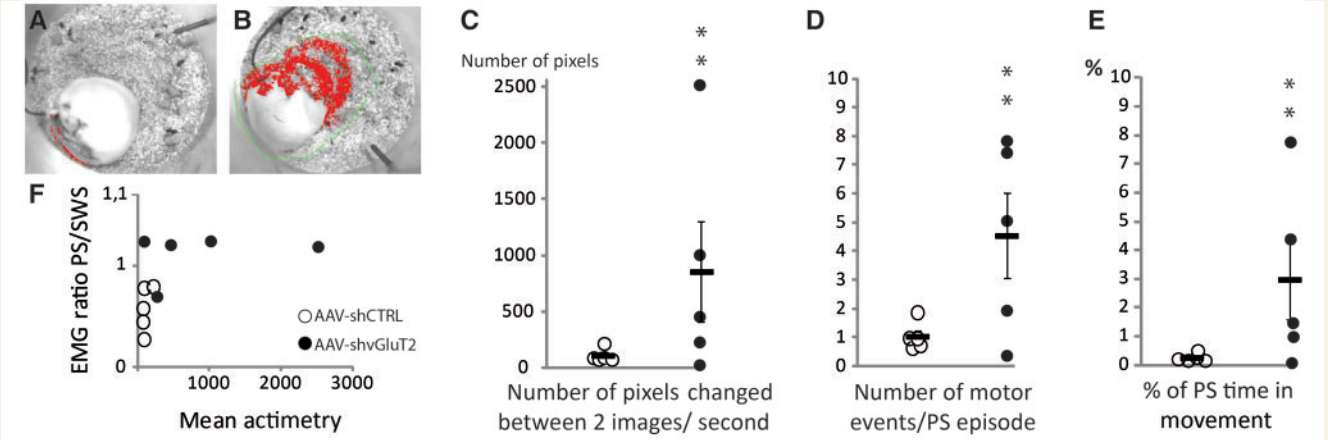

Figure 4 RBD-like behaviour episodes occur during paradoxical sleep after genetic inactivation of glutamate SLD neurons as evidenced by actimetry analysis. Examples of captured video images of representative AAV-shCTRL (**A**) and AAV-shvGluT2 rats (**B**), both during a paradoxical sleep episode. Each red point corresponds to a grey colour changed pixel between two successive images (see 'Materials and methods' section). The density and location of red points, respectively reflect intensity of rat's movements and body territories where they occurred. Actimetry thus shows that movements during paradoxical sleep are greatly enhanced in AAV-shvGluT2 (**B**) versus control (**A**) rats. (**C–E**) Dot plots comparing in AAV-shCTRL (open circles) and AAV-shvGluT2 (filled circles) rat either the mean actimetry per paradoxical sleep second (number of changed pixels between two captured images, **C**), the mean number of motor events per paradoxical sleep episode (**D**), and the percentage of paradoxical sleep time with rat's movements (**E**). Note that for the three calculated parameters, values are homogeneous and low in control rats and more variable and higher in experimental rats. (**F**) Dot plots showing no correlation between paradoxical sleep/slow-wave sleep EMG ratio and actimetry values. Non-parametric unpaired Mann-Whitney U-test, $^{*}P < 0.05$; $^{**}P < 0.01$ compared to AAV-shCTRL. SWS = slow-wave sleep.

Supplementary Videos 1–3). We objectively quantified abnormal oneiric, RBD-like behaviours by off-line 'actimetry' analysis of videos time-locked to polysomnography (Fig. 4A and B). We found out that the mean actimetry index (corresponding to the mean number of video pixels modified every second of paradoxical sleep) significantly increased in AAV-shvGluT2 versus AAV-shCTRL rats (Mann–Whitney U-test, $Z = -2.449$, $P = 0.01$; Fig. 4C). More precisely, both the number of motor events (5.6 ± 1.4 versus 1.0 ± 0.2; Mann–Whitney U-test, $Z = -2.449$, $P = 0.01$) and the percentage of paradoxical sleep with movements (3.7 ± 1.6 versus $0.3 \pm 0.1\%$; Mann–Whitney U-test, $Z = -2.449$, $P = 0.01$) significantly increased in experimental versus control rats (Fig. 4D and E). The careful observation of EMG signals and videos revealed a great variability in intensity and frequency of abnormal motor events among paradoxical sleep episodes in each experimental rat and within AAV-shvGluT2 group (Fig. 3G and H). Such variability between individuals has been reported in RBD patients (Oudiette *et al.*, 2009; Iranzo *et al.*, 2016). It is unlikely that it is due to a difference in the number or location of the glutamate SLD neurons inactivated as AAV injection sites included in this work are similar between rats. Rather, it could be due to stronger movements in some of them associated with more intense and vivid oneiric activities. Qualitatively, motor enactments during paradoxical sleep correspond to assorted non-elaborated behaviours that are loosely arranged at the level of the head, fore and hind limbs (Supplementary Video 2), tail or nose, rarely synchronized over multiple body territories. Occasional more complex movements were observed like seeking for food with the snout in woodchips, eating a virtual pellet, trying to run or jump (Supplementary Video 3). During these oneiric-like motor behaviours, experimental rats kept their eyes closed, indicating they are asleep. Vocalizations were not obvious in experimental rats. However, whether they emit ultrasonic vocalizations during paradoxical sleep remains to be studied using specific microphones. Experimental rats depicted normal locomotor activity and feeding behaviour during waking (with a standard weight increase) and did not display dream enactments during slow-wave sleep, seizures or modification of their body aspect.

Discussion

This work noticeably expands our knowledge on paradoxical sleep by deciphering at anatomical, genetic and functional levels the contribution of the SLD, considered for decades the paradoxical sleep generator. It can be functionally concluded from our results that the contingent of glutamate SLD neurons generates the paradoxical sleep-related muscle atonia and plays a limited role in paradoxical sleep generation. After genetic inactivation of glutamate, SLD signalling, paradoxical sleep is characterized by an increased muscle tone and the occurrence of abnormal excessive motor activities, resembling oneiric-like behaviours

of RBD patients. In support of these physiological results, our tract-tracing data reveal that glutamate SLD neurons selectively activated during paradoxical sleep send descending projections to the medullary structures containing the GABA/glycine inhibitory premotor neurons inducing muscle atonia but not to the intralaminar thalamus neurons known to mediate the activation of the cortex during paradoxical sleep.

To determine the physiological roles that play glutamate SLD neurons in paradoxical sleep, we used AAV-shRNAs to irreversibly impair glutamate release in SLD neurons, abolishing the expression of *Slc17a6*/vGluT2 mRNA and the presence of the protein in synaptic terminals. This method allows one to selectively inactivate glutamate neurons and not other types of SLD neurons, such as GABAergic and cholinergic neurons, in contrast to previously used cytotoxic lesions or local pharmacology (Sastre and Jouvet, 1979; Boissard *et al.*, 2002; Lu *et al.*, 2006). Further, the molecular tools used obviate the need for transgenic mice (Krenzer *et al.*, 2011) and can be applied in the rat, a species in which the anatomo-functional delimitation of the SLD has been finely decrypted (Maloney *et al.*, 2000; Boissard *et al.*, 2002, 2003; Lu *et al.*, 2006; Clement *et al.*, 2011; Boucetta *et al.*, 2014).

Experimental rats depicted during paradoxical sleep aberrant motor events absent in control animals, whereas these movements never occurred during slow-wave sleep and motor behaviour remained normal during waking. Similar motor manifestations likely corresponding to oneiric behaviours have been reported in transgenic $vGlut2^{flox/flox}$ mice after ablation of glutamate SLD signalling (Krenzer *et al.*, 2011) and in cats and rats with a lesion of SLD area (Sastre *et al.*, 1981; Lu *et al.*, 2006). However, in contrast to our work, the objective quantification of the muscle tone alterations and of the abnormal movements occurring during paradoxical sleep in experimental versus control animals were lacking in these previous studies. To address this, we developed and validated two complementary off-line analysis methods. First we considered nuchal EMG signal to compute the variation of muscle tone across the sleep–waking cycle. Second, we used video recordings to calculate an actimetric index of the rat's whole body reflecting every motor activity experienced during each paradoxical sleep episode. Taking advantage of these new tools, we were able to draw, for the first time, a precise paradoxical sleep-occurring behavioural phenotype in response to the genetic inactivation of glutamate transmission in the rat SLD neurons. Further, our results clearly show that glutamate SLD neurons generate the muscle atonia during paradoxical sleep.

Previous studies have shown that the electrocoagulation of the SLD in the cat or its neurochemical lesion with ibotenic acid in the rat reduced daily paradoxical sleep quantities to 40% of control levels by shortening individual bouts (Sastre *et al.*, 1981; Lu *et al.*, 2006). Here we show that the genetic inactivation of glutamate SLD neurons reduces by 33% the daily paradoxical sleep amounts due to a combined decrease in the number and duration of episodes. Comparable results were reported in transgenic $vGlut2^{flox/flox}$ mice with a bilateral injection of cre recombinase-expressing AAVs into the SLD and adjacent laterodorsal tegmentum to similarly eliminate local glutamate signalling (Krenzer *et al.*, 2011). Altogether, these data indicate that the glutamate SLD neurons are involved but not necessary for paradoxical sleep generation and EEG activation. This breaks the commonly accepted role of SLD neurons in paradoxical sleep generation, by means of simultaneous EEG activation through their ascending projections to intralaminar thalamus and a loss of muscle tone via their descending inputs to GABA/glycine premotor neurons in the gigantocellular reticular nucleus (Luppi *et al.*, 2011; Peever *et al.*, 2014). To provide an anatomical substratum of the present physiological data, we examined how SLD neurons interact with both intralaminar thalamus and gigantocellular reticular nucleus. We did not find any SLD neurons sending collaterals to both nuclei simultaneously. SLD neurons with ascending projections to the intralaminar thalamus do not express c-Fos during paradoxical sleep hypersomnia, in contrast to those projecting to the gigantocellular reticular nucleus, indicating the existence of two types of SLD neurons. We previously showed in rats that 84% of the c-Fos + neurons in SLD after paradoxical sleep hypersomnia express vGlut2 (Clement *et al.*, 2011). Further, most of the PS-on neurons recorded in the SLD were histochemically identified as glutamate in nature by combining juxtacellular recordings and double labelling in naturally sleeping-waking, head-fixed rats (Boucetta *et al.*, 2014). There is therefore no doubt that SLD descending neurons are glutamate, active during paradoxical sleep and functionally responsible for inducing muscle atonia during paradoxical sleep. Our results also suggest their contribution to the fine-tuning of paradoxical sleep regulation. One possibility to be explored is that the SLD contains two subpopulations of glutamate PS-on neurons, one group with descending projections, the other group that may innervate areas critically involved in paradoxical sleep. This is the case for the posterior hypothalamus and the ventrolateral part of the periaqueductal grey as supported by previous anterograde tract-tracing in rats (Boissard *et al.*, 2002). Moreover, both structures are interconnected, contain different populations of PS-on neurons and functionally control paradoxical sleep genesis (Verret *et al.*, 2006; Sapin *et al.*, 2009; Clement *et al.*, 2012; Luppi *et al.*, 2014). It is therefore likely that the removal in both areas of glutamate inputs from SLD in experimental rats may slightly unbalance this complex network with a limited deficit in paradoxical sleep amounts as a result.

The role in paradoxical sleep and the neurochemical nature of the SLD ascending projecting neurons to the intralaminar thalamus remain unclear. They could be GABA in nature since they are indeed present in SLD but do not express c-Fos after paradoxical sleep hypersomnia (Verret *et al.*, 2006; Sapin *et al.*, 2009). The selective inactivation of GABA neurotransmission in SLD neurons of

the transgenic $Vgat^{flox/flox}$ mice by local injection of AAV-cre did not result in any changes in paradoxical sleep suggesting that they do not play a role in paradoxical sleep (Krenzer *et al.*, 2011). Here we also found that almost a quarter of SLD neurons projecting to intralaminar thalamus are cholinergic in nature in lines with previous studies showing that cholinergic neurons in the dorsal pontine tegmentum including SLD project to the intralaminar thalamus (Woolf and Butcher, 1986; Hallanger *et al.*, 1987; Semba *et al.*, 1990). Pontine cholinergic neurons display a slow and tonic firing during both waking and paradoxical sleep and are nearly silent during slow-wave sleep (Boucetta *et al.*, 2014), suggesting that ascending SLD neurons belong to a larger group of pontine cholinergic cells with a promoting role in cortical activation during waking and paradoxical sleep (Luppi *et al.*, 2011; Brown *et al.*, 2012).

The effects on muscle and behavioural activity we observed and quantified when inactivating glutamate SLD neurons in rats recapitulate quite exactly the pathological profile of RBD patients. The inactivation of other structures connected to SLD as inhibitory gigantocellular reticular nucleus neurons or the central nucleus of amygdala likely involved in emotional content of dreams (Zhang *et al.*, 2012; Boucetta *et al.*, 2016) are needed to determine their potential contribution to muscle atonia during paradoxical sleep and RBD and thus to validate parallel animal models of RBD. The present preclinical model, as RBD patients, suffers loss of normal muscle paralysis during paradoxical sleep which results in abnormal and forceful dream enactments (Schenck *et al.*, 1986). As in humans, lack of muscle atonia is heterogeneous, quite variable between individuals and paradoxical sleep bouts. Moreover, RBD rats and humans never stand up during motor-enactment, and eyes stay closed. These symptomatic similarities in patients and rats suggest that damage to the SLD neurons may underlie this human disorder. Functional neuroimaging and post-mortem brain studies reported the presence of Lewy bodies, neuronal loss, depigmentation and/or gliosis within the coeruleus/subcoeruleus complex that broadly includes the SLD in idiopathic RBD patients (Schenck *et al.*, 1996; Boeve *et al.*, 2007; Arnulf, 2012; Boeve, 2013; Iranzo *et al.*, 2013), and neuronal loss strongly correlates with the severity of the motor symptoms (Garcia-Lorenzo *et al.*, 2013; Ehrminger *et al.*, 2016). Around 80% of patients suffering idiopathic RBD later develop a synucleinopathy such as Parkinson's disease (Arnulf, 2012; Howell and Schenck, 2015). Hence, idiopathic RBD is to date considered the best prodromal marker of such pathologies (Iranzo *et al.*, 2016). Data harvested so far in RBD patients and in our rat model strongly indicate that glutamate SLD neurons are required for the generation of muscle atonia during paradoxical sleep and play a limited role in the state of paradoxical sleep *per se*. These neurons may be initially targeted by α-synuclein-dependent pathological processes leading to their degeneration and/or malfunctioning in RBD patients, anticipating for years the diagnosis of synucleinopathies such as Parkinson's disease. As RBD patients do not show a decrease in paradoxical sleep quantities, we propose that only descending glutamate SLD neurons responsible for muscle atonia are targeted. Determining why and how the population of descending glutamate SLD neurons is selectively vulnerable is a challenging question of major scientific and clinical relevance that must be answered for a better understanding of RBD aetiology and the mechanisms responsible for its progressive conversion over years to synucleinopathies. Our convenient, stable (for weeks) and reproducible genetic rat model that mimics faithfully RBD motor symptoms offers an ideal way to develop new therapeutic strategies.

Acknowledgements

Warm thanks to Annabelle Bouchardon and Denis Ressnikoff from CIQLE facility for confocal microscopy and Sébastien Arthaud for his help with animals.

Funding

This work was supported by INSERM U1028, CNRS UMR5292 and Université Claude Bernard Lyon I. S.V.G. received PhD grants from Ministère de l'Education Supérieure et de la Recherche and the Fondation France Parkinson.

Supplementary material

Supplementary material is available at *Brain* online.

References

Arnulf I. REM sleep behavior disorder: motor manifestations and pathophysiology. Mov Disord 2012; 27: 677–89.

Arthaud S, Varin C, Gay N, Libourel PA, Chauveau F, Fort P, et al. Paradoxical (REM) sleep deprivation in mice using the small-platforms-over-water method: polysomnographic analyses and melanin-concentrating hormone and hypocretin/orexin neuronal activation before, during and after deprivation. J Sleep Res 2015; 24: 309–19.

Boeve BF. Idiopathic REM sleep behaviour disorder in the development of Parkinson's disease. Lancet Neurol 2013; 12: 469–82.

Boeve BF, Dickson DW, Olson EJ, Shepard JW, Silber MH, Ferman TJ, et al. Insights into REM sleep behavior disorder pathophysiology in brainstem-predominant Lewy body disease. Sleep Med 2007; 8: 60–4.

Boissard R, Fort P, Gervasoni D, Barbagli B, Luppi PH. Localization of the GABAergic and non-GABAergic neurons projecting to the sublaterodorsal nucleus and potentially gating paradoxical sleep onset. Eur J Neurosci 2003; 18: 1627–39.

Boissard R, Gervasoni D, Schmidt MH, Barbagli B, Fort P, Luppi PH. The rat ponto-medullary network responsible for paradoxical sleep onset and maintenance: a combined microinjection and functional neuroanatomical study. Eur J Neurosci 2002; 16: 1959–73.

Boucetta S, Cisse Y, Mainville L, Morales M, Jones BE. Discharge profiles across the sleep-waking cycle of identified cholinergic, GABAergic, and glutamatergic neurons in the pontomesencephalic tegmentum of the rat. J Neurosci 2014; 34: 4708–27.

Boucetta S, Salimi A, Dadar M, Jones BE, Collins DL, Dang-Vu TT. Structural brain alterations associated with rapid eye movement sleep behavior disorder in Parkinson's disease. Sci Rep 2016; 6: 26782.

Brown RE, Basheer R, McKenna JT, Strecker RE, McCarley RW. Control of sleep and wakefulness. Physiol Rev 2012; 92: 1087–187.

Clément O, Valencia Garcia S, Libourel PA, Arthaud S, Fort P, Luppi P-H. The inhibition of the dorsal paragigantocellular reticular nucleus induces waking and the activation of all adrenergic and noradrenergic neurons: a combined pharmacological and functional neuroanatomical study. PLoS One 2014; 9: e96851.

Clément O, Sapin E, Bérod A, Fort P, Luppi PH. Evidence that neurons of the sublaterodorsal tegmental nucleus triggering paradoxical (REM) sleep are glutamatergic. Sleep 2011; 34: 419–23.

Clément O, Sapin E, Libourel PA, Arthaud S, Brischoux F, Fort P, et al. The lateral hypothalamic area controls paradoxical (REM) sleep by means of descending projections to brainstem GABAergic neurons. J Neurosci 2012; 32: 16763–74.

Ehrminger M, Latimier A, Pyatigorskaya N, Garcia-Lorenzo D, Leu-Semenescu S, Vidailhet M, et al. The coeruleus/subcoeruleus complex in idiopathic rapid eye movement sleep behaviour disorder. Brain 2016; 139: 1180–8.

Fort, P, Bassetti CL, Luppi PH. Alternating vigilance states: new insights regarding neuronal networks and mechanisms. Eur J Neurosci 2009; 29: 1741–53.

Garcia-Lorenzo D, Longo-Dos Santos C, Ewenczyk C, Leu-Semenescu S, Gallea C, Quattrocchi G, et al. The coeruleus/subcoeruleus complex in rapid eye movement sleep behaviour disorders in Parkinson's disease. Brain 2013; 136: 2120–9.

Hallanger AE, Levey AI, Lee HJ, Rye DB, Wainer BH. The origins of cholinergic and other subcortical afferents to the thalamus in the rat. J Comp Neurol 1987; 262: 105–24.

Howell MJ, Schenck CH. Rapid eye movement sleep behavior disorder and neurodegenerative disease. JAMA Neurol 2015; 72: 707–12.

Iranzo, A. Management of sleep-disordered breathing in multiple system atrophy. Sleep Med 2005; 6: 297–300.

Iranzo A, Santamaria J, Tolosa E. Idiopathic rapid eye movement sleep behaviour disorder: diagnosis, management, and the need for neuroprotective interventions. Lancet Neurol 2016; 15: 405–19.

Iranzo A, Tolosa E, Gelpi E, Molinuevo JL, Valldeoriola F, Serradell M, et al. Neurodegenerative disease status and post-mortem pathology in idiopathic rapid-eye-movement sleep behaviour disorder: an observational cohort study. Lancet Neurol 2013; 12: 443–53.

Krenzer M, Anaclet C, Vetrivelan R, Wang N, Vong L, Lowell BB, et al. Brainstem and spinal cord circuitry regulating REM sleep and muscle atonia. PLoS One 2011; 6: e24998.

Lazarus M, Shen HY, Cherasse Y, Qu WM, Huang ZL, Bass CE, et al. Arousal effect of caffeine depends on adenosine A2A receptors in the shell of the nucleus accumbens. J Neurosci 2011; 31: 10067–75.

Lu J, Sherman D, Devor M, Saper CB. A putative flip-flop switch for control of REM sleep. Nature 2006; 441: 589–94.

Luppi PH, Clément O, Sapin E, Valencia Garcia S, Peyron C, Fort P. Animal models of REM dysfunctions: what they tell us about the cause of narcolepsy and RBD?. Arch Ital Biol 2014; 152: 118–28.

Luppi PH, Clément O, Sapin E, Gervasoni D, Peyron C, Léger L, et al. The neuronal network responsible for paradoxical sleep and its dysfunctions causing narcolepsy and rapid eye movement (REM) behavior disorder. Sleep Med Rev 2011; 15: 153–63.

Luppi PH, Fort P, Jouvet M. Iontophoretic application of unconjugated cholera toxin B subunit (CTb) combined with immunohistochemistry of neurochemical substances: a method for transmitter identification of retrogradely labeled neurons. Brain Res 1990; 534: 209–24.

Maloney KJ, Mainville L, Jones BE. Differential c-Fos expression in cholinergic, monoaminergic, and GABAergic cell groups of the pontomesencephalic tegmentum after paradoxical sleep deprivation and recovery. J Neurosci 1999; 19: 3057–72.

Maloney KJ, Mainville L, Jones BE. c-Fos expression in GABAergic, serotonergic, and other neurons of the pontomedullary reticular formation and raphe after paradoxical sleep deprivation and recovery. J Neurosci 2000; 20: 4669–79.

Mathis J, Hess CW, Bassetti C. Isolated mediotegmental lesion causing narcolepsy and rapid eye movement sleep behaviour disorder: a case evidencing a common pathway in narcolepsy and rapid eye movement sleep behaviour disorder. J Neurol Neurosurg Psychiatry 2007; 78: 427–9.

Oudiette D, De Cock VC, Lavault S, Leu S, Vidailhet M, Arnulf I. Nonviolent elaborate behaviors may also occur in REM sleep behavior disorder. Neurology 2009; 72: 551–7.

Paxinos G, Watson C. The rat brain atlas in stereotaxic coordinates. San Diego: Academic; 1998.

Peever J, Luppi PH, Montplaisir J. Breakdown in REM sleep circuitry underlies REM sleep behavior disorder. Trends Neurosci 2014; 37: 279–88.

Postuma RB, Gagnon JF, Vendette M, Montplaisir JY. Markers of neurodegeneration in idiopathic rapid eye movement sleep behaviour disorder and Parkinson's disease. Brain 2009; 132: 3298–307.

Renouard L, Billwiller F, Ogawa K, Clément O, Camargo N, Abdelkarim M, et al. The supramammillary nucleus and the claustrum activate the cortex during REM sleep. Sci Adv 2015; 1: e1400177.

Roussel B, Pujol J, Jouvet M. Effets des lésions du tegmentum pontique sur les états de sommeil chez le rat. Arch Ital Biol 1976; 1: 188–209.

Sakai K. Paradoxical (rapid eye movement) sleep-on neurons in the laterodorsal pontine tegmentum in mice. Neuroscience 2015; 310: 455–71.

Sakai K, Crochet S, Onoe H. Pontine structures and mechanisms involved in the generation of paradoxical (REM) sleep. Arch Ital Biol 2001; 139: 93–107.

Sakai K, Koyama Y. Are there cholinergic and non-cholinergic paradoxical sleep-on neurones in the pons?. Neuroreport 1996; 7: 2449–53.

Sapin E, Lapray D, Bérod A, Goutagny R, Léger L, Ravassard P. Localization of the brainstem GABAergic neurons controlling paradoxical (REM) sleep. PLoS One 2009; 4: e4272.

Sastre JP, Jouvet M. Le comportement onirique du chat. Physiol Behav 1979; 22: 979–89.

Sastre JP, Sakai K, Jouvet M. Are the gigantocellular tegmental field neurons responsible for paradoxical sleep?. Brain Res 1981; 229: 147–61.

Schenck CH. Rapid eye movement sleep behavior disorder: current knowledge and future directions. Sleep Med 2013; 14: 699–702.

Schenck CH, Bundlie SR, Ettinger MG, Mahowald M. Chronic behavioral disorders of human REM sleep: a new category of parasomnia. Sleep 1986; 9: 293–308.

Schenck CH, Bundlie SR, Mahowald MW. Delayed emergence of a parkinsonian disorder in 38% of 29 older men initially diagnosed with idiopathic rapid eye movement sleep behaviour disorder. Neurology 1996; 46: 388–93.

Scherfler C, Seppi K, Donnemiller E, Goebel G, Brenneis C, Virgolini I, et al. Voxel-wise analysis of [123I] β-CIT SPECT differentiates the Parkinson variant of multiple system atrophy from idiopathic Parkinson's disease. Brain 2005; 128: 1605–12.

Semba K, Reiner PB, Fibiger HC. Single cholinergic mesopontine tegmental neurons project to both the pontine reticular formation and the thalamus in the rat. Neuroscience 1990; 38: 643–54.

Thakker DR, Hoyer D, Cryan, JF. Interfering with the brain: use of RNA interference for understanding the pathophysiology of psychiatric and neurological disorders. Pharmacol Ther 2006; 109: 413–38.

Tippmann-Peikert M, Boeve B, Keegan BM. REM sleep behavior disorder initiated by acute brainstem multiple sclerosis. Neurology 2006; 66: 1277–79.

Vanni-Mercier G, Sakai K, Lin JS, Jouvet M. Mapping of cholinoceptive brainstem structures responsible for the generation of paradoxical sleep in the cat. Arch Ital Biol 1989; 127: 133–64.

Verret L, Fort P, Gervasoni D, Léger L, Luppi PH. Localization of the neurons active during paradoxical (REM) sleep and projecting to the locus coeruleus noradrenergic neurons in the rat. J Comp Neurol 2006; 495: 573–86.

Verret L, Léger L, Fort P, Luppi PH. Cholinergic and noncholinergic brainstem neurons expressing Fos after paradoxical (REM) sleep deprivation and recovery. Eur J Neurosci 2005; 21: 2488–504.

Woolf NJ, Butcher, LL. Cholinergic systems in the rat brain: III. Projections from the pontomesencephalic tegmentum to the thalamus, tectum, basal ganglia, and basal forebrain. Brain Res Bull 1986; 16: 603–37.

Zhang J, Xi M, Fung SJ, Sampogna S, Chase MH. Projections from the central nucleus of the amygdala to the nucleus pontis oralis in the rat: an anterograde labeling study. Neurosci Lett 2012; 525: 157–62.